



Title	A chromatic transient visual evoked potential based encoding/decoding approach for brain-computer interface
Author(s)	Lai, SM; Zhang, Z; Hung, YS; Niu, Z; Chang, C
Citation	IEEE Journal on Emerging and Selected Topics in Circuits and Systems, 2011, v. 1 n. 4, p. 578-589
Issued Date	2011
URL	http://hdl.handle.net/10722/155731
Rights	IEEE Journal on Emerging and Selected Topics in Circuits and Systems. Copyright © Institute of Electrical and Electronics Engineers

A Chromatic Transient Visual Evoked Potential Based Encoding/Decoding Approach for Brain–Computer Interface

Sui Man Lai, *Member, IEEE*, Zhiguo Zhang, *Member, IEEE*, Yeung Sam Hung, *Senior Member, IEEE*, Zhendong Niu, and Chunqi Chang, *Member, IEEE*

Abstract—This paper presents a new encoding/decoding approach to brain–computer interface (BCI) based on chromatic transient visual evoked potential (CTVEP). The proposed CTVEP-based encoding/decoding approach is designed to provide a safer and more comfortable stimulation method than the conventional VEP-based stimulation methods for BCI without loss of efficiency. For this purpose, low-frequency isoluminant chromatic stimuli are time-encoded to serve as different input commands for BCI control, and the superior comfortableness of the proposed stimulation method is validated by a survey. A combination of diversified signal processing techniques are further employed to decode the information from CTVEP. Based on experimental results, a properly designed configuration of the CTVEP-based stimulation method and a tailored signal processing framework are developed. It is demonstrated that high performance (at information transfer rate: 58.0 bits/min, accuracy: 94.9%, false alarm rate: 1.3%) for BCI can be achieved by means of the CTVEP-based encoding/decoding approach. It turns out that to achieve such good performance, only simple signal processing algorithms with very low computational complexity are required, which makes the method suitable for the development of a practical BCI system. A preliminary prototype of such a system has been implemented with demonstrated applicability.

Index Terms—Brain–computer interface (BCI), chromatic transient visual evoked potential, electroencephalography, time-encoded visual stimulation.

I. INTRODUCTION

BRAIN–COMPUTER interface (BCI) is an emerging technology which provides a direct communication pathway between brain and computer without muscle activity and thus it allows people who are completely or severely paralyzed to reestablish communication with the world [1]–[4]. Due to the highly noisy and nonstationary nature of brain signals, the encoding and decoding of brain signals for BCI are challenging

problems and most reported methods are still not very efficient. Hence, BCIs are considered to be devices with relatively low communication bandwidth. Most BCIs have maximum information transfer rate (ITR) up to 25 bits/min [4]–[6], although a few exogenous BCIs, which require user's sensation abilities to elicit sensory electrophysiological activities, can achieve higher ITRs. For example, steady-state visual evoked potential (SSVEP)-based BCI [7] and flash onset and offset visual evoked potential (FVEP)-based BCI [8] can achieve as high as 51.5 bits/min and 34 bits/min, respectively. For these VEP-based BCIs to support high ITRs, the visual stimuli used such as LED flashes and checkerboard reversal are often modulated by high-frequency (6–30 Hz) flickering [9] and/or luminance variation. Flickering stimuli in such high frequency range may evoke epileptic seizures [10] and fast-varying luminance of stimuli can easily fatigue and exhaust users [11]. Consequently, extensive application of existing VEP-based BCI is hampered by its uncomfortable user experience and safety concerns. Hence, it is highly desirable to be able to deliver visual stimuli to users of VEP-based BCIs in a more comfortable and safer manner. To this end, we propose a new encoding/decoding approach based on chromatic transient visual evoked potential (CTVEP), instead of SSVEP and FVEP, for BCI.

CTVEPs are elicited when chromatic visual stimuli are presented at low frequency (<4 Hz) and perceived within the visual field. As shown in Fig. 1, CTVEPs are characterized by the absence of positive C_I deflection, and the presence of negative C_{II} deflection and C_{III} deflection in a typical onset/offset transient VEP waveform, where C_I and C_{II} are responsible for isochromatic luminance and isoluminant chromatic modulation respectively [13]–[16]. Isoluminant chromatic stimulus with low frequency stimulation can elicit stronger transient CTVEPs through chromatic modulation compared with luminance modulation. To the best of our knowledge, no medical report indicates that such stimulation may evoke epileptic seizures or other medical symptoms. Hence, the potential problems of luminance modulation related fatigue and epileptic seizure triggering, encountered in almost all of the SSVEP-based and FVEP-based BCIs, can be avoided. The safety of the proposed approach is due to low frequency change in the visual stimulation on the one hand, and no luminance variation on the other hand.

With low frequency change and no luminance variation in the visual stimulation, our proposed CTVEP-based BCI is expected to be more comfortable for users than the conventional

Manuscript received June 15, 2011; revised October 31, 2011; accepted November 08, 2011. Date of publication December 22, 2011; date of current version February 01, 2012. This work was supported by GRF under Grant HKU_762111M of Hong Kong RGC, in part by National 973 project 2012CB720702 of China, in part by University of Hong Kong Seed Funding Programme for Applied Research (200902160038), and in part by the University of Hong Kong Small Project Funding (201007176335). This paper was recommended by Guest Editor J. Sanchez.

S. M. Lai, Z. Zhang, Y. S. Hung, and C. Q. Chang are with the Department of Electrical and Electronic Engineering, The University of Hong Kong, Pokfulam, Hong Kong (e-mail: cqchang@eee.hku.hk).

Z. Niu is with School of Computer Science and Technology, Beijing Institute of Technology, Beijing 100081, China.

Digital Object Identifier 10.1109/JETCAS.2011.2178734

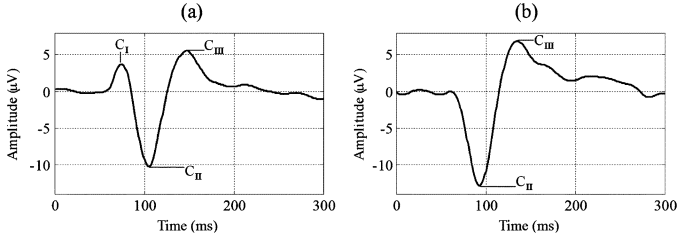


Fig. 1. (a) A typical pattern onset/offset transient VEP waveform, three main components (C_I , C_{II} , and C_{III}) recommended by the International Society for Clinical Electrophysiology of Vision (ISCEV) [12] are indicated. (b) A representative CTVEPs obtained from one of the subjects elicited by isoluminant chromatic stimuli. In comparison with (a), C_I is absent while C_{II} and C_{III} can be clearly observed in (b).

SSVEP-based and FVEP-based BCIs. To validate this claim, we have conducted a survey among fourteen subjects recruited in the experimental study of this paper. In this survey the subjects are asked to choose the most preferable stimulus among four types of isoluminant chromatic stimuli and a simple black/white stimulus used in luminance modulation based BCI. The survey result shows that all subjects prefer isoluminant stimulus with 2 cycles per degree (cpd) circular grating as the most comfortable and easiest to focus on. Meanwhile, all subjects ranked the simple white/black stimulus to be the least preferable one as it easily caused fatigue.

In this paper, based on chromatic modulated CTVEPs, we firstly propose a new encoding technique, in which isoluminant chromatic stimuli are time-encoded into different codes to serve as different input commands for BCI control. In particular, we 1) design a suitable isoluminant chromatic stimulus which gives an optimized CTVEP response; 2) develop a time-encoded visual stimulation method based on the designed stimulus for BCI applications; 3) evaluate the performance of the developed stimulation method with experiments; 4) design, implement, and test a preliminary BCI prototype system based on the proposed novel CTVEP encoding/decoding approach. Through these investigations, we demonstrate that CTVEPs of good signal quality can be elicited with proper stimulus design and can be encoded temporally to provide multiple distinguishable combinations for supporting multiple BCI commands. Further, we develop a decoding technique to utilize a combination of signal processing and pattern recognition techniques for translating CTVEPs into BCI commands. Experimental results show that the proposed time-encoded CTVEP-based BCI performs very well with high ITR, high accuracy, and low false alarm rate. It turns out that to achieve such good performance, only simple signal processing algorithms with very low computational complexity are required, which makes the method suitable for the development of a practical BCI system.

The rest of the paper is organized as follows. Section II briefly introduces the mechanism of CTVEP generation and stimulation parameters which contribute to the quality of CTVEP. Experimental design for developing the CTVEP-based encoding/decoding approach is introduced in Sections III. Section IV is devoted to establish a complete signal analysis framework for the CTVEP-based encoding/decoding approach. Experimental results and comparisons are presented in Section V. Section VI

presents the design, implementation, and testing of a preliminary BCI prototype system based on the proposed novel CTVEP encoding/decoding approach. Discussions and conclusions are finally given in Section VII.

II. STIMULATION PARAMETERS OF CTVEPS

In this section, we introduce a series of stimulation parameters that affect the quality of CTVEPs and then describe ways to elicit CTVEPs with optimal signal quality.

Locations: Same as other VEPs, CTVEPs are stronger when the stimulus is located at the center of the visual field than at periphery, which is known as the “cortical magnification” phenomenon due to the uneven cone cell distribution in the retina [17], [18].

Spatiotemporal conditions: Robust CTVEP responses can be elicited by isoluminant chromatic grating with appropriate spatiotemporal conditions. In human visual system, there are two types of visual pathways, magnocellular (M) and parvocellular (P), which show considerable functional overlap, and chromatic information is mainly handled by the P pathway [19]–[21]. By choosing proper spatial and temporal stimulation parameters, the functional separation between M and P pathways is maximized and the corresponding chromatic cortical responses can be optimized [22]. Studies have demonstrated that CTVEPs elicited by pattern onset/offset approach give more robust responses than pattern reversal approach [14], [23], which may be due to reduction in behaviour of the brain called adaptation phenomenon [24], [25]. It is also recommended in [14] to choose a duty cycle less than or around 20% to give distinctive CTVEP response. On the other hand, other studies have shown that, under onset/offset presentation, isoluminant chromatic sinusoidal gratings with spatial frequencies 0.5–2 cpd could give a robust CTVEP response [13], [26], [27].

Color Opponent: In human visual system, color opponent transformation is done by color opponent cells in retina for visual processing. Based on color opponent theory, there are four different single opponent cells: red on/green off (+L/−M), green on/red off (+M/−L), green on/blue off (+M/−S) and blue on/green off (+S/−M), and two double opponent cells: red–green on/red–green off (L−M/−(L−M)) and yellow–blue on/yellow–blue off ((L+M)−S/−((L+M)−S)). L, M, and S correspond to long, middle, short wavelengths, respectively; positive and negative signs mean on and off center arrangement of the opponent cells, respectively. There are three fundamental opponent pairs in color space to match human visual color opponent system, which are also known as color constancy. They include black–white (LUM) pair, red–green (LM) pair, and blue–yellow (S) pair. In this paper, we choose red–green pair for stimulus design, as it can be presented in an isoluminant mode to reduce luminance flickering related fatigue while black–white pair is equivalent to luminance-modulation and blue–yellow pair gives less robust and longer transient VEP response [13], [14]. Besides, studies have shown that increasing the contrast between red and green will elicit more robust CTVEPs with larger amplitude and shorter latency, and it becomes saturate at high contrast level [14], [26], [28]. Therefore, in this paper, we design the stimuli with the highest

contrast level that our display units can afford to maximize CTVEP responses.

In the next section, we describe the experiments to select the optimal stimulation parameters, including spatial frequencies, spatial arrangements of stimulation, double-opponent or single-opponent stimulation, etc.

III. EXPERIMENTAL DESIGN

Two experiments were conducted with the aim to design the CTVEP-based decoding/encoding approach for BCI control. Experiment 1 was to design isoluminant chromatic stimuli with appropriate spatiotemporal parameters to give optimized CTVEP responses by varying spatial frequencies and arrangements of the stimuli. Experiment 2 was to study and evaluate the performance with the designed time-encoded CTVEP visual stimulation method under different configurations, include: double-opponent stimuli (DOS) and single-opponent stimuli (SOS), adaptive averaging (AA), and nonadaptive averaging (NAA), and different combinations of spatial filters used in subsequent decoding processes. Based on the results of the two experiments, we could find the most effective configurations of decoding/encoding for the CTVEP-based BCI.

A. Visual Stimuli

Isoluminant chromatic sinusoidal gratings were presented on a DiamondDigital DV998FDB 19-in Flat CRT color monitor. Graphical control was managed by ATI Radeon X1300 graphic card. The monitor refreshing rate was 85 Hz and resolution of the screen was 1280×960 pixels, equivalent to $27^\circ \times 20^\circ$.

In Experiment 1, the stimuli used were isoluminant red–green horizontal or circular sinusoidal grating with spatial frequencies, 0.33, 1, 2, 4, 8 cpd, which varied within each subset of experiment and they were presented at the center of the screen with 3° diameter, having a small black dot as fixation center.

In Experiment 2, according to both the investigation of signal quality in Experiment 1, as shown in Section V-A later, and the survey on comfortableness as described in Section I, for the sake of optimal signal quality and user comfortableness, isoluminant red–green circular sinusoidal gratings with 2 cpd of spatial frequency were used as stimuli for performance study of DOS, while isoluminant pure red/green filled circles were used as stimuli for performance study of SOS. Fig. 2(a) and (b) show the appearance of DOS and SOS respectively. For both studies, six stimuli with 3° diameter each were presented at six locations as shown in Fig. 2, and each of them had a small black dot as fixation center.

In both experiments, stimuli were spatially low-pass filtered at 10 cpd to minimize chromatic aberration [21], [29], [30]. A color ratio $r = 0.5$, defined by red luminance to sum of red and green luminance $\{\text{red}/(\text{red}+\text{green})\}$, was used to provide pure color contrasting without luminance intrusion. This ratio was chosen to closely match to human equiluminant point [31]. In CIE XYZ coordinate system, red is defined as $x = 0.406, y = 0.287$; green as $x = 0.223, y = 0.374$ and the mean is $x = 0.314, y = 0.330$ with a mean luminance of 20 cd/m^2 , where (x, y) represents the chromaticity coordinate in CIE 1931 XYZ color space.

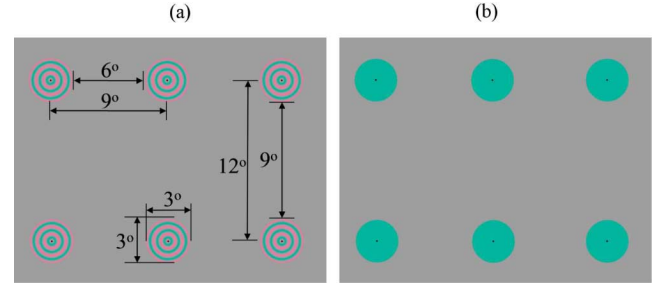


Fig. 2. Appearance and position of (a) DOS, (b) SOS presented on the screen. Except for the color of stimuli in (b) being different from (a), other specifications in (b) are the same as illustrated in (a).

In pattern onset/offset presentation for both experiments, stimuli were turned on for 47 ms and turned off for 200 ms, resulting in a duty cycle of 19%. A complete onset/offset cycle with a duration of 247 ms denoted a code of “1,” while one silent cycle with a duration of 247 ms denoted a code of “0.” As a result, a 4-bit “1-1-0-0” code would take 988 ms ≈ 1 s to complete.

B. EEG Recording

Electroencephalography (EEG) was recorded binocularly using a NeuroScan Quik-cap electrode placement system with 12 and 19 Ag/AgCl electrodes in Experiment 1 and Experiment 2, respectively. International 10/10 electrode placement standard was followed for electrode positioning [32]. Twelve Ag/AgCl scalp electrodes (FCz, PO3, POz, PO4, O1, Oz, O2, I1, Iz, I2 for active recording, Cz for grounding and Fz for referencing) and nineteen Ag/AgCl scalp electrodes (FCz, Pz, PO7, PO3, POz, PO4, PO8, PO9, O1, Oz, O2, PO10, I1, Iz, I2, T7, T8 for active recording, Cz for grounding and Fz for referencing) were used in Experiments 1 and 2, respectively. Fig. 3 shows the position of electrodes used in Experiment 2. All electrodes used were kept at an impedance of less than 5 k Ω and monitored under the built-in impedance measurement module. Signals were recorded using two synchronized NeuroScan SynAmps RT amplifiers (Compumedics NeuroScan, El Paso, TX,) and signal analysis was done through SCAN 4.3 (NeuroScan) and MATLAB 7.7 (Mathworks, Natick, MA). In both experiments, EEG signals were continuously recorded, filtered (0.05–200 Hz, -3 dB/oct , single pole), amplified 15 folds and digitized at a sampling rate of 1 kHz with 24 bit resolution.

In Experiment 1, once the data were collected from each subject, they were bandpass filtered at 1–40 Hz using a FIR filter with a specification of -96 dB/oct and zero phase shift and segmented into 600 of 1000 ms epochs in total for 10 subsets of experiment. Bipolar spatial filtering by subtracting Oz with either O1 or O2 was used to enhance signal-to-noise ratio (SNR). Each subset of experiment was formed by 20 segments. Each segment consisted of a notification sound at first. After 0.5 s, three consecutive “1-1-0-0” presentations were presented with a notification sound right at the end, followed by 1.5 s resting. Thus, the total time taken for each segment was approximately 5 s. Eventually, 60 epochs (20 segments and three individual “1-1-0-0” presentations per segment) were collected for each subset of the

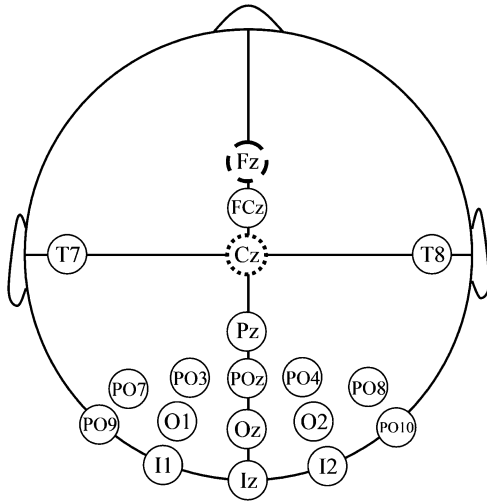


Fig. 3. Position of electrodes used in the performance studies for DOS and SOS. Solid circles represent active electrodes while dotted and dashed circles represent reference (Cz) and ground electrode (Fz), respectively.

experiment. Ten subsets of the experiment for horizontal and circular gratings, with spatial frequencies at 0.33, 1, 2, 4, and 8 cpd, were collected for each subject. The background was kept with the same mean chromaticity and luminance (20 cd/m^2), and with the same small black fixation at the center throughout the experiment. Calibration was done with Spyder3 Elite and CHY 631 lightmeter. Viewing distance was 76 cm and stimuli were viewed binocularly.

In Experiment 2, EEG data under the same bandpass filtering configuration as in Experiment 1 were segmented into 720 of 1000 ms epochs in total for twelve subsets of experiment. Six subsets of data with six corresponding codes were used as training data and another six subsets of data were used as testing data. Their roles would be swapped for two-fold cross validation. For unipolar referencing, we analyzed signals from Oz. For bipolar filtering, we analyzed signals from Oz subtracted by one of the electrodes: O1, O2, PO7, or PO8. For other filtering techniques, we used all 17 active electrodes for signal processing. Six 4-bit codes (0-0-1-1, 0-1-0-1, 0-1-1-0, 1-0-0-1, 1-0-1-0, 1-1-0-0) were adopted and presented simultaneously. In each set of experiments, subjects were instructed to focus at one of the corresponding codes. In total, 12 subsets of experiments for six codes (two subsets of experiments for each code) were collected for each subject. Other experimental parameters used were the same as described in Experiment 1.

C. Rationale for Codes Selection

Theoretically, the possible number of inputs is the integral numbers of bit used to the power of two, i.e., 4-bit binary encoding scheme has 16 different codes, represented in binary operation. Although using all 16 codes might achieve a high information transfer rate (ITR), in practice the tradeoff will be low accuracy and high false alarm rate (FAR) and thus result in low ITR. This can be reasoned as follows. Codes with one “1” or no “1” are hard to be distinguished from background brain activities which has a code of 0-0-0-0, while codes with large number of “1s” (three “1s” or four “1s”) are hard to be distinguished

from each other and other codes with two “1s”. In addition, codes with more “1s” are more vulnerable to brain adaptation phenomena (i.e., CTVEP signals may have weaker responses after prolonged exposure). It is desirable to choose a subset of codes which have reasonably large distance from each other. For this purpose we can use a subset of codes with two “1s” in the 4-bit binary encoding scheme, i.e., the six 4-bit codes described above. It can be easily verified that the distance between any pair of these six selected codes is either 2 or 4, i.e., 2 or 4 bits different from each other. In addition, they have also a distance of 2 to the background code 0-0-0-0. We might also include the code 1-1-1-1 since it has a distance of 2 to all the six codes with two “1s” and a distance of 4 to the background code. However, since it is easier to arrange six codes on the screen than seven codes, and the 1-1-1-1 code with four “1s” may be more vulnerable to brain adaptation phenomena, we finally choose only the six codes with two “1s” to achieve a good tradeoff between number of control inputs and quality of input signals.

D. Subjects

In Experiment 1, EEG data were collected from four subjects (four males, age range 21–24 years). In Experiment 2, EEG data were collected from 14 subjects (11 males and 3 females, age range 21–28 years, mean = 23 ± 2 years) for performance study with DOS and five subjects (five males, age range 21–24 years) for performance study with SOS. All subjects had normal or corrected vision of $\geq 20/20$ Snellen visual acuity and were classified as normal color vision by the Ishihara test and the Farnsworth–Munsell 100-Hue test. No previous ocular or systemic disease was reported for these subjects. Subjects were seated at a comfortable chair and experiments were done in a dim, unshielded office laboratory with reasonable activities to simulate real-life situation. Subjects were instructed to gaze at the fixation after the first notification sound, minimizing their eye blinking, and to rest after the second notification sound. A short break of about 45 s–1 min between two consecutive subsets of experiment was given to subjects for the purpose of resting.

IV. SIGNAL PROCESSING

A. Matched Filter and Inter-Epoch Analysis for Experiment 1

We first adopted two approaches: matched filter analysis and inter-epoch analysis, to determine the optimal stimulation parameters for eliciting CTVEPs based on the data recorded in Experiment 1.

A matched filter or a template was the average of 60 epochs in one subset of experiment. The quality of a matched filter was evaluated by SNR, where the “signal” and “noise” were respectively the recorded data in signal window (“1-1”) and noise window (“0-0”). A matched filter with a higher SNR would perform better when it was used as a template for BCI classification.

Inter-epoch analysis is an alternative approach to compare the quality of CTVEPs. The 60 epochs in one subset of experiment were partially averaged across three consecutive epochs, resulting in 20 inter-averaged epochs. We next analyzed the quality of these three-fold inter-averaged epochs under different

spatial frequencies and arrangements in terms of three parameters: SNR, C_{II} -to- C_{III} amplitude, and C_{II} -to- C_{III} latency consistency. C_{II} -to- C_{III} amplitudes were the differences between amplitudes of C_{II} and C_{III} (see Fig. 1), and they were normalized for each subject by the maximum value of each subject. Latencies, referring to the time point of C_{II} in CTVEP, reflected the durations of VEP responses after stimulation for each subject, and they were normalized by subtracting the minimum latency of each subject. Smaller variation in the latency distribution meant higher consistency of CTVEP responses. All the three parameters were important for choosing suitable stimulation parameters. For an inter-averaged epoch with higher SNR, or/and larger C_{II} -to- C_{III} amplitude, or/and higher latency consistency with its corresponding matched filter, it would have a higher correlation with the correct matched filter and lower correlation with other unrelated matched filters and noise.

One-way ANOVA and Tukey's Honestly Significant Differences (HSD) post-hoc test were performed to determine the effect of spatial frequency with different grating arrangement on the SNR of the "1-1-0-0" three-fold inter-averaged epochs. ANOVA was used to test for existence of any mean difference between multiple group distributions while Tukey's HSD post-hoc test technique was used afterward to locate which groups were contributing to the differences.

B. Feature Extraction and Classification for Experiment 2

We next proposed a signal processing framework for decoding the EEG signals into output commands associated with the user's intention. The decoding framework consisted of several modules including: temporal filtering, adaptive averaging, spatial filtering, matched filtering and feature classification, as seen in Fig. 4. In short, temporal filtering, adaptive averaging and spatial filtering were used to improve the SNR of the signal of interest. Matched filtering was used to recognize the signals by comparing the extracted signal with appropriate templates. Feature classification was used to classify the extracted features into proper classes.

1) *Nonadaptive Averaging and Adaptive Averaging:* Averaging is the simplest and most commonly used method to improve the quality of event-related EEG signals [33]. Upon across-epoch averaging, coherent signals will be retained while incoherent signals and noise will be suppressed. Due to the inherent classification speed-accuracy tradeoff for system involving averaging, the number of averaging epochs per classification depends largely on the requirement of the BCI application.

In this paper, we tested two different averaging approaches to improve the SNR of the CTVEPs: nonadaptive averaging (NAA) and adaptive averaging (AA). The NAA approach was to average a fixed number of epochs per classification, and the optimal number was determined in the training phase as the one having the best BCI performance. The AA approach was to average a variable number of epochs per classification, which depended on the classification result right after each epoch was processed. More precisely, when an epoch was collected and processed, the classification would immediately be done and be used to determine whether further averaging was necessary. If the classifier gave a confident result (the correlation coefficient

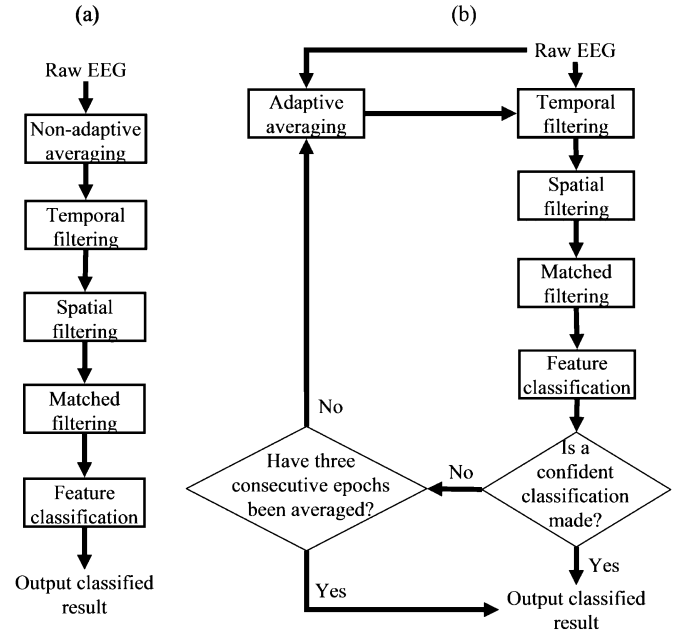


Fig. 4. Signal processing flow charts when using (a) NAA or (b) AA approaches in the time-encoded CTVEP visual stimulation method for BCI.

between the filtered signals and only one of the matched filters was above the thresholding), the classification was finished and the result would be sent out as the control command for BCI. If the classifier did not give a confident result, the next epoch would be averaged into the previous epoch to improve the SNR. Then the classifier would proceed with this averaged epoch to make a new classification. The process would be executed iteratively until a confident result was obtained or three epochs (the maximum number of epochs used in the averaging) had been averaged. If the final result did not give a confident result, the system returned an unclassified state called "Idle." Else, the system returned a classified state labeled with the corresponding control command. Fig. 4(a) and (b) show the signal flow charts of NAA and AA approaches, respectively.

2) *Temporal Filtering:* The purpose of temporal filtering is to improve the quality of EEG signals by removing unrelated signals and noise beyond the frequencies of interest. We used a FIR bandpass filter with a passband of 1–40 Hz as the temporal filter.

3) *Spatial Filtering:* The purpose of spatial filtering is to improve EEG signal quality by removing unrelated signals and noise according to their spatial distribution across different electrodes. We implemented several spatial filtering techniques and their different possible combinations. Their performances were evaluated and compared using datasets of Experiment 2. Fig. 5 illustrates the three stages of spatial filters and six spatial filtering techniques under test. In total 20 physically meaningful combinations of these spatial filters were studied.

The first stage spatial filters included bipolar and common average referencing (CAR). Bipolar derivation derived the first spatial derivative between two inputs to enhance differences in the voltage gradient in one direction and also removed correlated noise. CAR derived the spatial derivative between inputs and the averaged template of these inputs, in order to remove

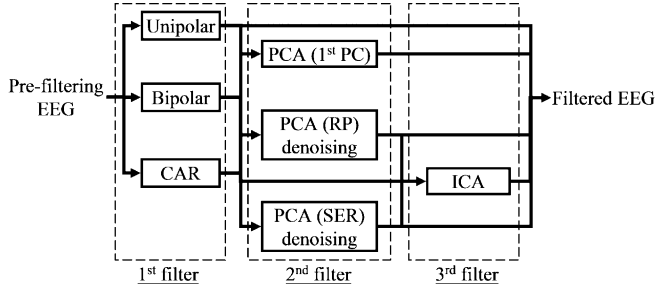


Fig. 5. Signal flow chart of spatial filters. Six spatial filtering techniques with unipolar referencing are categorized into three stages (first, second, third stage filters).

the correlated noise across these inputs and suppress uncorrelated noise [34]. Unipolar referencing was also considered in the first stage filter as a control measurement.

The second stage spatial filters were principal component analysis (PCA) based filtering and they include three alternatives. PCA-1stPC decomposed inputs into different principal components (PC) and reconstructed a single output according to the most dominant PC with respect to its power. The PCA-RP (residual power) denoising and PCA-SER (selective eigen-rate) denoising reconstructed outputs with the same numbers of inputs by removing PCs but with different criteria. PCA-RP removed PCs that accounted for the least 5% eigen-values [35], while PCA-SER removed eigen-value sorted PCs that had differences of normalized consecutive eigen-value no more than a chosen threshold [36].

The third stage spatial filter was independent component analysis (ICA). ICA performed decomposition of inputs into a set of independent components (IC) and the most suitable IC was chosen as output automatically by comparing ICs with all matched filters. Matched filtering is discussed in the following.

4) *Matched Filtering*: The purpose of matched filtering is to find the corresponding template having the best correlation with the EEG signals and thereby to reveal the user intention. Matched filtering based on zero-lag cross-correlation coefficients was performed to decode the EEG signals by comparing them with matched filters (templates) for different codes. A higher correlation coefficient implied a better matching to the user's intention. In the training phase, six 4-bit codes with 60 epochs were collected from each subject. Then, different matched filters were obtained for different codes through coherent averaging.

Fig. 6 shows the experimental results of different matched filters in the 4-bit coding scheme for CTVEPs, each with 60 epochs averaged. In the figure the mean and standard deviation of the 60 epochs of EEG signals are plotted. Since the standard deviation seems large in the plot, we must clarify that this is the standard deviation of the 60 raw signals. However, the standard deviation of the estimated CTVEP templates should be $\sqrt{60}$ (~ 7.7) times lower. Therefore the estimates of the CTVEP templates are actually quite reliable.

5) *Feature Classification*: After correlation coefficients of the EEG epochs were extracted, we used a simple thresholding approach to classify them into the correct class for device control. For each classification, a set of correlation coefficients were

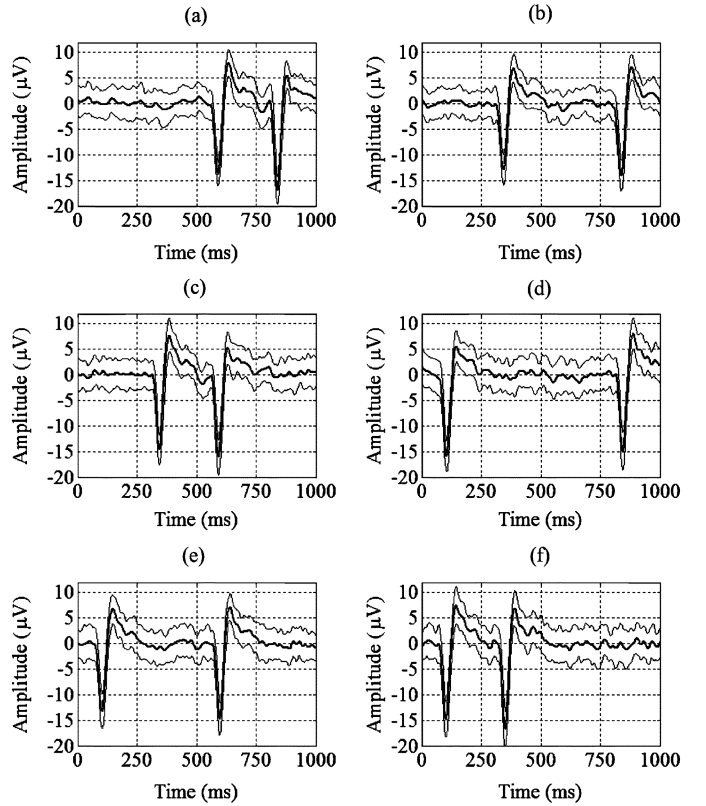


Fig. 6. Matched filter plots for all six codes: (a) 0-0-1-1, (b) 0-1-0-1, (c) 0-1-1-0, (d) 1-0-0-1, (e) 1-0-1-0, (f) 1-1-0-0 under the designed 4-bit coding scheme. CTVEPs in all of these matched filters were elicited by pattern onset/offset isoluminant red-green circular 2 cpd sinusoidal gratings (DOS). Each matched filter was obtained by averaging 60 epochs with the same code. Mean and ± 1 S.D. of the 60 epochs of EEG signals are indicated by thick and thin lines, respectively.

returned from matched filtering, a threshold would then be applied to classify them. If there was only one coefficient exceeding the threshold, the result would be classified into the corresponding class. Otherwise, the result would be classified into a null class called “idle state.” As classes of stimuli during training phase were known, we could find the best threshold for correlation coefficients by comparison between target and non-target data groups. Afterwards, we could find the optimal local threshold of each code from the population and then could obtain a global threshold by averaging all local thresholds. In our experiments, we found that different local thresholds were similar to each others when enough samples were provided. Finally, this global threshold was used to classify unknown testing data that were independent of the training data and performance evaluation was done based on the classification results. This classification approach was simple and suitable for real time implementation, and it achieved a satisfactory BCI performance in our experiments.

C. Performance Measures

1) *Information Transfer Rate*: For performance measurement of communication and control systems, the information transfer rate (ITR) was used to provide an objective performance indicator with consideration of both accuracy and speed [37], [38]. For a BCI with M possible selections and a command

classification accuracy of P , we assumed that it had the same selection probability P for each desired selection and selection probability $(1 - P)/(M - 1)$ for each undesired selection. Then the bit rate B for each decision can be expressed as

$$B = \log_2 M + P \log_2 P + (1 - P) \log_2 \left[\frac{1 - P}{M - 1} \right]. \quad (1)$$

ITR would then be calculated by dividing bit rate B by command transfer interval (CTI), which is defined as the ratio between the total experimental time (expressed in minute) and the total number of command decisions made during this period of time.

2) *Accuracy and False Alarm Rate*: Accuracy is defined as the number of correct classifications divided by the total number of classifications. The false alarm rate (FAR) is defined as the number of misclassifications (apart from idle state) divided by the total number of classifications. Consequently, accuracy and FAR can be described as the probability of making correct classification and the probability of making wrong classification apart from idle state. It is important to evaluate both accuracy and FAR. For example, higher accuracy will improve the reliability of the BCI and lower FAR will decrease the chance of controlling the BCI with a wrong command, both of which are crucial to a high-precision and error-intolerable system.

D. Performance Evaluation

In Experiment 2, classification results were evaluated to estimate the performance, based on training and testing data sets collected, in terms of ITR, accuracy and FAR. These measures were used to evaluate the performance using different configurations including AA and NAA approaches, and different combinations of spatial filters, under DOS based time-encoded CTVEP visual stimulation.

V. RESULTS

A. Experiment 1: Choice of a Suitable Visual Stimulus

1) *Matched Filter Analysis*: We found that SNR under both circular and horizontal stimulus presentations exhibited similar bandpass characteristics, as shown in Fig. 7. A relatively high SNR was found at 2–4 cpd and SNR drops beyond this range. At 2–4 cpd for both circular and horizontal stimuli, similar SNR values were obtained, ranging from 13.7–16.1 dB. For higher spatial frequency of 8 cpd, the average SNR was 8.6 dB. For lower spatial frequency, the average SNR was 11.1 dB for 1 cpd and 8.6 dB for 0.33 cpd. These findings are consistent with similar studies showing bandpass characteristics of the VEP signal strength when spatial frequency is varied [14], [26], and suggest that when the isoluminant chromatic sinusoidal grating is designed with spatial frequency of 2 or 4 cpd, either circular or horizontal arrangement can give a relatively good quality of matched filtering.

2) *Inter-Epoch Analysis*: Firstly, we analyzed SNR of epochs with different spatial configurations (Fig. 8). One-way ANOVA revealed that SNR was not significantly different between circular and horizontal gratings with 2 and 4 cpd ($p = 0.192$). However, ANOVA followed by HSD post-hoc test revealed that SNRs of these four configurations (circular 2,

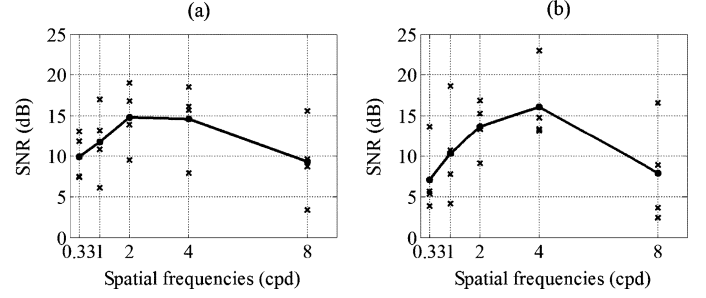


Fig. 7. SNR plots of “1-1-0-0” matched filter with (a) circular and (b) horizontal isoluminant chromatic sinusoidal gratings as a function of spatial frequency.

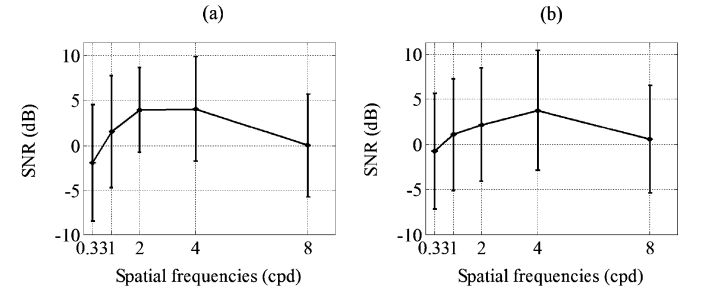


Fig. 8. SNR plots of “1-1-0-0” partially averaged epoch with (a) circular and (b) horizontal isoluminant chromatic sinusoidal gratings as a function of spatial frequency. Error bars indicate ± 1 S.D.

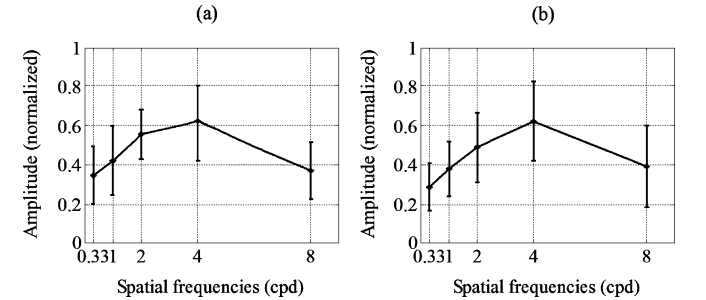


Fig. 9. Normalized amplitude plots of “1-1-0-0” partially averaged epoch for the first stimulation with (a) circular, (b) horizontal as a function of spatial frequency. Error bars indicate ± 1 S.D.

4 cpd and horizontal 2, 4 cpd) were significantly greater than other grating arrangements with different spatial frequencies ($p = 0.015$). This concludes that these four configurations are relatively better than their counterparts in term of SNR.

Secondly, we analyzed the C_{II} -to- C_{III} amplitude and latency consistency of different spatial configurations, respectively (Figs. 9 and 10). We found that the results showed bandpass spatial tuning characteristic with the C_{II} -to- C_{III} amplitudes peaked at 2–4 cpd for both circular and horizontal gratings and diminished below 2 cpd and above 4 cpd, and a U-shape characteristic with shorter latencies at 1–4 cpd and longer beyond this region.

Lastly, for both gratings, normalized C_{II} -to- C_{III} amplitudes and latencies were not significantly different between the first and the second CTVEPs in “1-1-0-0” epochs with the same spatial frequency respectively ($p = 0.063$ and $p = 0.132$), suggesting that both C_{II} -to- C_{III} amplitude and latency of CTVEP

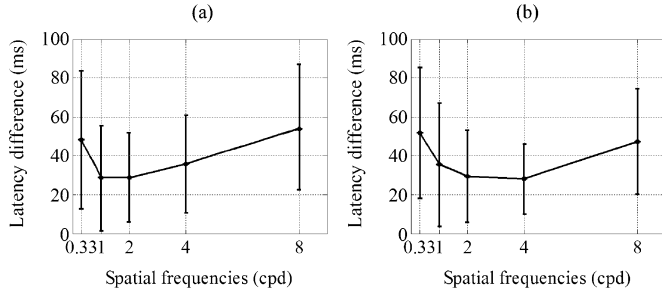


Fig. 10. Normalized latency difference plots of “1-1-0-0” partially averaged epoch for the first stimulation with (a) circular, (b) horizontal gratings. Latencies were normalized by subtracting the minimum latency of each subject from their VEP latencies. Error bars indicate ± 1 S.D.

TABLE I

SUMMARY OF THE THREE PERFORMANCE MEASURES FOR DOS WITH AA AND NAA APPROACHES, AND DIFFERENT FIRST STAGE SPATIAL FILTERS

1st Spatial filter	ITR (bits/min)		Accuracy (%)		FAR (%)	
	AA	NAA	AA	NAA	AA	NAA
Unipolar	37.9 \pm 20.1	14.8 \pm 11.8	81.9 \pm 16.7	57.0 \pm 17.5	4.6 \pm 4.9	2.3 \pm 2.0
Bipolar	58.0 \pm 14.4	35.1 \pm 16.8	94.9 \pm 6.5	83.6 \pm 10.8	1.3 \pm 1.7	0.2 \pm 0.4
CAR	44.8 \pm 24.0	20.3 \pm 12.8	84.0 \pm 20.8	66.7 \pm 20.6	3.8 \pm 5.9	1.4 \pm 1.8

TABLE II

SUMMARY OF THE THREE PERFORMANCE MEASURES FOR SOS WITH AA AND NAA APPROACHES, AND DIFFERENT FIRST STAGE SPATIAL FILTERS

1st Spatial filter	ITR (bits/min)		Accuracy (%)		FAR (%)	
	AA	NAA	AA	NAA	AA	NAA
Unipolar	10.2 \pm 7.7	2.5 \pm 3.8	52.5 \pm 14.2	25.8 \pm 22.2	11.6 \pm 2.9	9.5 \pm 6.8
Bipolar	19.8 \pm 16.8	6.6 \pm 9.2	64.9 \pm 19.0	38.6 \pm 30.9	7.7 \pm 5.9	8.0 \pm 8.9
CAR	12.5 \pm 12.2	2.0 \pm 3.5	54.9 \pm 17.2	24.7 \pm 19.3	10.3 \pm 5.2	8.0 \pm 6.2

elicited by the second presentation of the stimulus were not different from the first presentation under the spatiotemporal parameters used.

B. Experiment 2: Performance of CTVEP-Based Encoding/Decoding

1) *Performance Study With DOS and SOS*: The same performance evaluation procedures were used in performance study with DOS and SOS. For SOS, as we intended to give a pilot and brief comparison with DOS, we would only show the results but would not include statistical analysis for them due to limited sample sizes (five subjects).

To compare different 1st stage spatial filters, the performance measures in terms of ITR, accuracy and FAR, were summarized in Tables I and II for DOS and SOS, respectively. Bipolar filtering gave a significantly ($p < 0.001$, Wilcoxon signed rank test) better performance when compared with unipolar referencing. Yet, CAR filtering did not show significantly ($p = 0.118$, Wilcoxon signed rank test) better performance.

However, when we considered these performance measures (ITRs shown in Fig. 11, but accuracy and FAR not shown to save space), for DOS and SOS with NAA, and DOS with AA, we found that applying any combinations of second and third stage spatial filters did not improve the performance, in comparison with the corresponding performance without the second

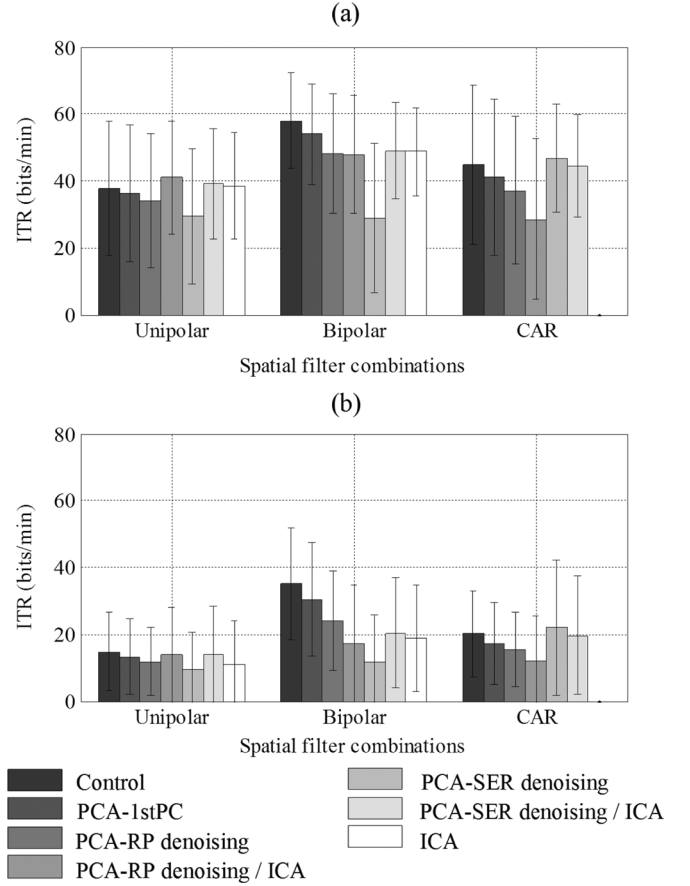


Fig. 11. In double-opponent stimulus presentation, ITR with different spatial filter combinations across fourteen subjects for (a) adaptive averaging and (b) nonadaptive averaging approaches are summarized above. Data are grouped into three main categories according to different first stage spatial filters. Data in each group correspond to different combinations of second and third stage spatial filters. Error bars indicate ± 1 S.D.

and/or third stage spatial filter. For SOS with AA, applying spatial filters based on PCA denoising followed by ICA or pure ICA might give better performance than without using any second or/and third stage spatial filter.

In terms of ITR and accuracy for both DOS and SOS, we found that AA performed significantly better than NAA ($p < 0.008$, Wilcoxon signed rank test) when only the 1st stage spatial filter is employed. In term of FAR, for both DOS and SOS, it was inconclusive to tell whether AA performed significantly better than NAA. The statistical results of DOS are summarized in Table III.

With DOS, the optimal numbers of averaging epochs were 1.6 ± 0.3 and 2.0 ± 1.0 for AA and NAA, respectively; whereas with SOS, the optimal numbers of averaging epochs were 2.0 ± 0.1 and 2.0 ± 1.0 for AA and NAA, respectively. In addition, when NAA approach was used, we found that, as the number of averaging epochs increased, the accuracy would increase, the ITR and FAR would decrease and approach zero.

From all these results, the following findings provide the basis for our recommendations on decoding processes for DOS:

- 1) any combination of the second and third stage spatial filters did not improve the performance;

TABLE III

STATISTICAL ANALYSIS SUMMARY OF THE THREE PERFORMANCE MEASURES OF DOS WITH AA AND NAA APPROACHES, AND DIFFERENT FIRST STAGE SPATIAL FILTERS

	<i>p</i> value (Wilcoxon signed rank test, N = 14)					
	ITR (bits/min)		Accuracy (%)		FAR (%)	
	AA	NAA	AA	NAA	AA	NAA
Bipolar vs unipolar	<0.001*	<0.001*	<0.001*	<0.001*	<0.001*	<0.001*
CAR vs unipolar	0.295	0.118	0.426	0.118	0.305	0.287
	AA vs NAA		AA vs NAA		AA vs NAA	
Unipolar	<0.001*		0.003*		0.009*	
Bipolar	<0.001*		<0.001*		0.033*	
CAR	0.003*		0.008*		0.188	

TABLE IV

COMPARISON OF THE MEAN OF ITR, ACCURACY, FAR, AND THE NUMBER OF AVERAGING EPOCHS BETWEEN DOS AND SOS PRESENTATIONS UNDER AA AND NAA APPROACHES

Stimuli used	Mean ITR (bits/min)		Mean accuracy (%)		Mean FAR (%)		Mean number of averaging	
	AA	NAA	AA	NAA	AA	NAA	AA	NAA
DOS (N = 14)	58.0	35.1	94.9	83.9	1.3	0.2	1.64	2
SOS (N = 5)	19.8	6.6	64.9	38.6	7.7	8.0	2.03	2
Difference	38.1	28.6	30.0	45.0	-6.4	-7.8	-0.39	0
<i>p</i> value	0.003*	0.003*	0.003*	0.002*	0.003*	0.148	0.003*	0.768

Wilcoxon rank sum testing was used to evaluate the significance of performance improvement of DOS over SOS. N is the number of samples used to determine the statistical results.

- 2) bipolar filtering gave significantly better performance than unipolar referencing but CAR filtering did not;
- 3) adaptive averaging performed significantly better than non-adaptive averaging.

2) *Comparison Between DOS and SOS:* Here, we only chose to apply bipolar spatial filtering technique for both types of stimuli to facilitate a fair comparison. We did the comparison based on three performance measures, namely: ITR, accuracy, and FAR, and the number of averaging for both AA and NAA approaches.

Under the AA approach, all performance measures and the numbers of averaging showed that DOS gave a significantly better performance than SOS (ITR: $p < 0.003$, accuracy: $p < 0.003$, FAR: $p < 0.003$, number of averaging: $p < 0.003$, Wilcoxon rank sum test). The results are summarized in Table IV. When DOS was compared against SOS, there was an increase of 38.1 bits/min in mean ITR, an increase of 30.0% in mean accuracy, a decrease of 6.4% in mean FAR and a decrease of 0.39 epochs in the mean number of averaging.

Under the NAA approach, two performance measures (ITR and accuracy) showed that DOS gave a significantly better performance than SOS (ITR, $p < 0.003$, accuracy, $p < 0.002$, Wilcoxon rank sum test). On the other hand, FAR and the number of averaging did not show a significant improvement in performance. When DOS was compared against SOS, there was an increase of 28.6 bits/min in mean ITR, an increase of 45.0% in mean accuracy, a decrease of 7.8% in mean FAR and without any difference in the mean number of averaging.

VI. DESIGN AND IMPLEMENTATION OF A PRACTICAL SYSTEM

We suggest that the proposed BCI method can be applied to, but not limited to, word processing system, internet browsing system, clinical communication system, gaming system, etc. For example, word entry can be achieved by choosing the designated letter or word through menu-based selection with all possible selections inside the selection hierarchy.

The practical implementation of the proposed CTVEP BCI system consists of four major components: 1) visual stimuli presentation of double-opponent circular grating as shown in Fig. 2(a), 2) acquisition of EEG signals, 3) online real-time command detection using the signal processing techniques proposed in this paper including preprocessing, feature extraction, and classification, and 4) control of external devices in particular applications under consideration as discussed above.

The novelty here lies in the proof of feasibility of the proposed BCI protocol for development of a practical, cost-effective and portable BCI prototype. In contrast to the commercial Compumedics Neuroscan system which is expensive, bulky and suitable only for offline research purpose, the prototype to be implemented is portable, low-cost, and capable of realtime processing. This however can only be achieved by a compromise in the signal quality of the prototype in comparison with that of the Neuroscan system.

A. Stimuli Presentation and Triggering System

In the experimental study reported in Section V, the stimulation is presented by the STIM (Compumedics Neuroscan, El Paso, TX) system using a CRT monitor. STIM provides synchronization information from parallel port of the computer, which is encoded in a way the SCAN 4.3 (Neuroscan) EEG acquisition system can identify. For a practical BCI system, we need to develop our own visual stimulation system. The visual stimulation control software is developed using Microsoft DirectX and C++ programming language, while the stimuli are presented on a LCD monitor instead of CRT. LCD monitor is more convenient and readily available, though it may not perform as good as CRT in VEP measurement. The frequency of the LCD monitor used in our prototype is 60 Hz. Using DirectX, visual stimulation is synchronized with the refresh rate of the monitor. For each bit of stimulation (an onset of a double-opponent circular grating stimulation), the stimulation picture is presented for three refresh cycles followed by 12 refresh cycles of silence, i.e., 50 ms stimulus presentation and 200 ms background presentation. These result in a 250 ms onset/offset duration with a duty cycle of 20%, which is close to the parameters (247 ms and 19%, respectively) used in the experimental study. The same six 4-bit codes as used in the experimental study are adopted in the BCI prototype, and the arrangement of the six codes on the monitor is also the same as shown in Fig. 2(a).

A most important issue is to synchronize visual stimulation with EEG signal acquisition, because coherent averaging of CTVEP is required for both AA and NAA. To this end, we output a trigger signal from the visual stimulation computer. The trigger, synchronized with the onset of visual stimulus, is an electrical signal output from the USB port of the computer and measured by the EEG signal acquisition device.

B. Signal Acquisition Unit

For the sake of portability, cost effectiveness, and online real-time acquisition in the prototype, we use a simple 16-bit two-channel bio-signal acquisition device made in-house, with common mode rejection ratio (CMRR) greater than 98 dB and a sampling rate of 1 kHz. The device has a USB interface through which the data can be read into a computer. One channel is used to record EEG signal at position Oz on the head, and the other channel is used to record the trigger signal outputted from the visual stimulation system.

C. Signal Processing System

As BCI is a real-time communication system, computational complexity of the signal processing techniques used is an important consideration. As demonstrated by the results of the experimental study and shown in Section V, the decoding framework recommended in this study only includes bipolar filtering, matched filtering and averaging across a small number of epochs, and its complexity is actually very low. We do not use signal processing techniques, such as PCA and ICA, which require a large amount of computational resources, as they do not offer better performance in our CTVEP encoding/decoding protocol. Therefore, the complexity is not an issue for our BCI prototype. Due to the low computation complexity, the signal processing can be implemented on a MCU chip, FPGA, portable mobile computing device such as iPhone. In our current prototype, however, for the ease of implementation, we use a personal computer, and the EEG signals are read from the signal acquisition unit and analyzed using MATLAB.

D. Result and Discussion

The practical BCI prototype has been tested on one young male subject, and Experiment 2 of the experimental study is repeated for this subject using the prototype. For each of the six 4-bit codes, 60 epochs of CTVEP signals are collected and averaged to obtain the CTVEP template used for matched filtering. The six averaged CTVEP templates for this subject are shown in Fig. 12.

Although the result of the BCI prototype is not as good as that shown in Fig. 6 obtained using the commercial Neuroscan EEG measurement system, it is evident that the six codes of the CTVEP templates are readily recognizable. Therefore, the BCI prototype should work for this subject.

The preliminary result on the BCI prototype, in addition to the encouraging experimental study, further demonstrates the practical applicability of a novel safe and comfortable BCI system based on our proposed CTVEP encoding/decoding method, with potentially high ITR.

VII. DISCUSSION AND CONCLUSION

A. Development Summary

In the optimal isoluminant chromatic stimulus determination study of Experiment 1, we found that for 3° red–green isoluminant chromatic sinusoidal grating with onset/offset presentation (duty cycle: 20%, period: 250 ms), both circular and horizontal gratings with spatial frequencies at 2–4 cpd gave relatively strong and consistent CTVEP responses. Under consider-

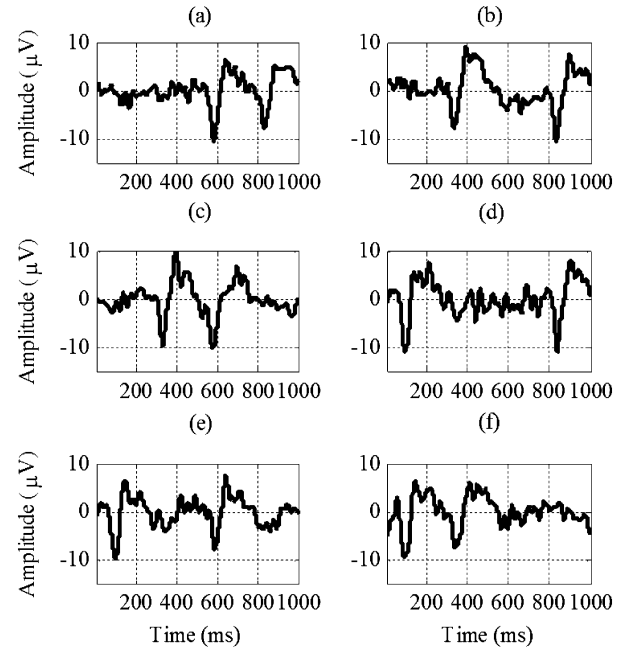


Fig. 12. Averaged CTVEP templates over 60 epochs for all six 4-bit codes for the subject tested using the BCI prototype: (a) 0-0-1-1, (b) 0-1-0-1, (c) 0-1-1-0, (d) 1-0-0-1, (e) 1-0-1-0, (f) 1-1-0-0; CTVEPs were elicited by pattern onset/offset isoluminant red–green circular 2cpd sinusoidal gratings (DOS).

ations of both objective and subjective aspects, circular grating with 2 cpd is recommended.

In the performance evaluation study of Experiment 2, we determined the best configurations for BCI control. We found that using double opponent stimuli with the combination of bipolar filtering and AA gave a significant improvement in performance over other stimulation configurations and signal processing techniques. Subsequently, we suggest applying six 3° isoluminant chromatic red/green sinusoidal 2 cpd gratings as stimuli for six commands, together with a decoding framework consisting of bipolar spatial filtering, adaptive averaging and matched filtering to give the best performance.

The average, the peak and the worst performance measures for fourteen subjects are summarized in Table V. From these results, we conclude that these configurations can achieve high performance and is suitable for potential BCI applications.

B. Future Directions

1) *Online Performance Evaluation*: Evaluation of online performance is an important experimental research direction to provide an objective measurement for the practical performance of the proposed method, and thereby to give a more precise and accurate picture of suitable BCI applications. Due to the presence of feedback in online BCI control, performance measured in online evaluation may be different from offline evaluation found by our study reported in this paper. It would be a very challenging task to assess the objective performance when the user controls the system freely. Typically, BCI performance can be assessed by asking subjects to control designed evaluation protocol. As a result, it is important to design the online evaluation protocol to match the online BCI control scenario as closely as possible.

TABLE V
SUMMARY OF PERFORMANCE MEASURES UNDER ISOLUMINANT
CHROMATIC 2 CPD GRATINGS, BIPOLAR FILTERING, ADAPTIVE
AVERAGING AND MATCHED FILTERING TECHNIQUES

	Performance measures		
	Average	Peak	Worst
ITR (bits/min)	58.0 \pm 14.4	75.3	24.9
Accuracy (%)	94.9 \pm 6.5	99.9	75.8
FAR (%)	1.3 \pm 1.7	0.0	6.0

2) *K-Bit CTVEP Encoding*: We have determined the optimal visual stimuli and electrode layout for the CTVEP-based BCI. Furthermore, we have developed a new CTVEP encoding technique to encode user intentions into EEG by presentation of stimuli with different timings to provide different codes for BCI control. From the results of our study and knowledge in the field, we determined that duration for each bit should be 0.25 s to allow enough presentation time of a distinctive CTVEP while minimizing the delay between presentations of consecutive bits, i.e., maximum bit-repetition frequency is 4 Hz.

In this study, we have designed a 4-bit encoding scheme and six corresponding codes were chosen 1) to maximize inter-stimulus and artifact separation, 2) to minimize brain adaptation phenomenon and, 3) to maximize the number of inputs. From the experimental results, we found that the proposed time encoding approach could give high performance for BCI control.

To further improve the proposed method when used in BCI control, increasing the number of inputs can directly boost the performance. Although this action inherently decreases the speed of the system, it may be compensated and make a positive contribution to ITR. This can be achieved by generalizing the 4-bit CTVEP encoding considered in this paper into K -bit CTVEP encoding where K is a positive integer. Based on the considerations of inter-stimulus separation, artifact separation, brain adaptation phenomenon and numbers of inputs, we suggest that the number of stimulating bits ("1") and the number of non-stimulating bits ("0") should be identical or close in a K -bit CTVEP encoding scheme.

3) *Advanced Feature Extraction and Classification*: Since essential information is encoded in the EEG signals, it is important to develop advanced feature extraction techniques to extract information effectively. In this study, we have shown that the matched filtering can extract features effectively. Apart from this, Common Spatial Pattern (CSP), wavelet transform, and other advanced signal processing techniques have been shown to be effective in several BCI applications [39]–[45]. As time-encoded CTVEPs carry certain distinguishable information in time and frequency domains, it is worth studying the suitability of the proposed methods and other possible techniques for feature extraction.

An effective classifier serves as a key to provide fast and accurate classification using the extracted features. As the distribution of correlation coefficients extracted from matched filtering appears to be classifiable effectively by linear classifiers and these classifiers require relatively low computational resources, it is worthwhile to explore the practical applicability of linear classification in the proposed method for BCI control. Other

classification methods like support vector machine (SVM) and neural network classifiers have been previously studied by other BCI research groups and shown to be useful for different BCI designs [46]–[50]. It is worthwhile to explore their performance and suitability as well in the future.

To conclude, we have studied and designed a new encoding and decoding approach for high performance BCI control based on CTVEPs that offers a simple, safe, user-friendly and comfortable solution to BCI control. A preliminary BCI prototype based on this method has been developed with demonstrated applicability. Since these advantages are essential for a successful and widely-applicable BCI design, we hope that the contributions in this paper will eventually lead to the development of a mature practical BCI system that benefits people with needs for such a system.

REFERENCES

- [1] J. R. Wolpaw, N. Birbaumer, D. J. McFarland, G. Pfurtscheller, and T. M. Vaughan, "Brain-computer interfaces for communication and control," *Clin. Neurophysiol.*, vol. 113, pp. 767–791, Jun. 2002.
- [2] G. Schalk, D. J. McFarland, T. Hinterberger, N. Birbaumer, and J. R. Wolpaw, "BCI2000: A general-purpose brain-computer interface (BCI) system," *IEEE Trans. Biomed. Eng.*, vol. 51, no. 6, pp. 1034–1043, Jun. 2004.
- [3] B. Z. Allison, E. W. Wolpaw, and J. R. Wolpaw, "Brain-computer interface systems: Progress and prospects," *Expert Rev. Med. Devices*, vol. 4, pp. 463–474, Jul. 2007.
- [4] B. Z. Allison, "Toward Ubiquitous," in *Brain-Computer Interfaces: Revolutionizing Human-Computer Interaction*, B. Graimann, B. Z. Allison, and G. Pfurtscheller, Eds., 1st ed. Berlin, Germany: Springer, 2011, pp. 357–387.
- [5] J. R. Wolpaw *et al.*, "Brain-computer interface technology: A review of the first international meeting," *IEEE Trans. Rehabil. Eng.*, vol. 8, no. 2, pp. 164–173, Jun. 2000.
- [6] T. M. Vaughan *et al.*, "Brain-computer interface technology: A review of the second international meeting," *IEEE Trans. Neural Syst. Rehabil. Eng.*, vol. 11, no. 2, pp. 94–109, Jun. 2003.
- [7] S. Parini, L. Maggi, A. C. Turconi, and G. Andreoni, "A robust and self-paced BCI system based on a four class SSVEP paradigm: Algorithms and protocols for a high-transfer-rate direct brain communication," *Comput. Intell. Neurosci.*, p. 864564, 2009.
- [8] P. L. Lee, J. C. Hsieh, C. H. Wu, K. K. Shyu, and Y. T. Wu, "Brain computer interface using flash onset and offset visual evoked potentials," *Clin. Neurophysiol.*, vol. 119, pp. 605–616, Mar. 2008.
- [9] D. Regan, *Human Brain Electrophysiology: Evoked Potentials and Evoked Magnetic Fields in Science and Medicine*. New York: Elsevier, 1989.
- [10] R. S. Fisher *et al.*, "Photic- and pattern-induced seizures: A review for the epilepsy foundation of America working group," *Epilepsia*, vol. 46, pp. 1426–1441, Sep. 2005.
- [11] M. Nomura, "A comfortable brain-interface to video displays," *Neural Netw.*, vol. 12, pp. 347–354, Mar. 1999.
- [12] J. V. Odom *et al.*, "Visual evoked potentials standard (2004)," *Doc. Ophthalmol.*, vol. 108, pp. 115–123, Mar. 2004.
- [13] C. Gerth, P. B. Delahunt, M. A. Crognale, and J. S. Werner, "Topography of the chromatic pattern-onset VEP," *J. Vis.*, vol. 3, pp. 171–182, 2003.
- [14] J. Rabin, E. Switkes, M. Crognale, M. E. Schneek, and A. J. Adams, "Visual evoked potentials in three-dimensional color space: Correlates of spatio-chromatic processing," *Vis. Res.*, vol. 34, pp. 2657–2671, Oct. 1994.
- [15] J. J. Kulikowski, I. J. Murray, and N. R. A. Parry, *Electrophysiological Correlates of Chromatic-Opponent and Achromatic Stimulation in Man*. New York: Academic, 1989.
- [16] T. A. Berninger, G. B. Arden, C. R. Hogg, and T. Frumkes, "Separable evoked retinal and cortical potentials from each major visual pathway: Preliminary results," *Br J. Ophthalmol.*, vol. 73, pp. 502–511, Jul. 1989.
- [17] C. A. Curcio, K. R. Sloan, R. E. Kalina, and A. E. Hendrickson, "Human photoreceptor topography," *J. Comp. Neurol.*, vol. 292, pp. 497–523, Feb. 22, 1990.
- [18] D. R. Williams, "Topography of the foveal cone mosaic in the living human eye," *Vis. Res.*, vol. 28, pp. 433–454, 1988.

- [19] I. J. Murray and J. J. Kulikowski, "VEPs and contrast," *Vis. Res.*, vol. 23, pp. 1741–1743, 1983.
- [20] J. J. Kulikowski, A. G. Robson, and D. J. McKeefry, "Specificity and selectivity of chromatic visual evoked potentials," *Vis. Res.*, vol. 36, pp. 3397–3401, Nov. 1996.
- [21] J. J. Kulikowski, *On the Nature of Visual Evoked Potentials, Unit Responses and Psychophysics*. New York: Plenum, 1991.
- [22] S. Tobimatsu, H. Tomoda, and M. Kato, "Human VEPs to isoluminant chromatic and achromatic sinusoidal gratings: Separation of parvocellular components," *Brain Topogr.*, vol. 8, pp. 241–243, 1996.
- [23] S. P. Heinrich and M. Bach, "Adaptation dynamics in pattern-reversal visual evoked potentials," *Doc. Ophthalmol.*, vol. 102, pp. 141–156, Mar. 2001.
- [24] A. Bradley, E. Switkes, and K. De Valois, "Orientation and spatial frequency selectivity of adaptation to color and luminance gratings," *Vis. Res.*, vol. 28, pp. 841–856, 1988.
- [25] C. Blakemore and F. W. Campbell, "On the existence of neurons within the human visual system selectively sensitive to the orientation and size of retinal images," *J. Physiol.*, vol. 203, no. 1, pp. 237–260, 1969.
- [26] V. Porciatti and F. Sartucci, "Normative data for onset VEPs to red-green and blue-yellow chromatic contrast," *Clin. Neurophysiol.*, vol. 110, pp. 772–781, Apr. 1999.
- [27] I. J. Murray, N. R. A. Parry, D. Garden, and J. J. Kulikowski, "Human visual evoked potentials to chromatic and achromatic gratings," *Clin. Vis. Sci.*, vol. 1, pp. 231–244, 1987.
- [28] G. S. Souza, B. D. Gomes, C. A. Saito, M. da Silva Filho, and L. C. Silveira, "Spatial luminance contrast sensitivity measured with transient VEP: Comparison with psychophysics and evidence of multiple mechanisms," *Invest. Ophthalmol. Vis. Sci.*, vol. 48, pp. 3396–3404, Jul. 2007.
- [29] D. I. Flitcroft, "The interactions between chromatic aberration, defocus and stimulus chromaticity: Implications for visual physiology and colorimetry," *Vis. Res.*, vol. 29, pp. 349–360, 1989.
- [30] J. J. Kulikowski, D. J. McKeefry, and A. G. Robson, "Selective stimulation of colour mechanisms: An empirical perspective," *Spat. Vis.*, vol. 10, pp. 379–402, 1997.
- [31] A. Fiorentini, V. Porciatti, M. C. Morrone, and D. C. Burr, "Visual ageing: Unspecific decline of the responses to luminance and colour," *Vis. Res.*, vol. 36, pp. 3557–3566, Nov. 1996.
- [32] M. R. Nuwer *et al.*, "IFCN standards for digital recording of clinical EEG. international federation of clinical neurophysiology," *Electroencephalogr. Clin. Neurophysiol.*, vol. 106, pp. 259–261, Mar. 1998.
- [33] A. Mouraux and G. D. Iannetti, "Across-trial averaging of event-related EEG responses and beyond," *Magn. Reson. Imag.*, vol. 26, pp. 1041–1054, Sep. 2008.
- [34] K. A. Ludwig *et al.*, "Using a common average reference to improve cortical neuron recordings from microelectrode arrays," *J. Neurophysiol.*, vol. 101, pp. 1679–1689, Mar. 2009.
- [35] I. T. Jolliffe, *Principal Component Analysis*. New York: Springer-Verlag, 1986.
- [36] S. Andrews, R. Palaniappan, and N. Kamel, "Extracting single trial visual evoked potentials using selective eigen-rate principal components," in *World Acad. Sci., Eng. Technol.*, 2005.
- [37] C. E. Shannon, "The mathematical theory of communication. 1963," *MD Comput.*, vol. 14, pp. 306–317, Jul.–Aug. 1997.
- [38] J. R. Pierce, *An Introduction to Information Theory*. New York: Dover, 1980.
- [39] L. Qin and B. He, "A wavelet-based time-frequency analysis approach for classification of motor imagery for brain-computer interface applications," *J. Neural Eng.*, vol. 2, pp. 65–72, Dec. 2005.
- [40] G. Dornhege *et al.*, "Combined optimization of spatial and temporal filters for improving brain-computer interfacing," *IEEE Trans. Biomed. Eng.*, vol. 53, no. 11, pp. 2274–2281, Nov. 2006.
- [41] L. Song and J. Epps, "Classifying EEG for brain-computer interface: Learning optimal filters for dynamical system features," *Comput. Intell. Neurosci.*, p. 57180, 2007.
- [42] Q. Zhao and L. Zhang, "Temporal and spatial features of single-trial EEG for brain-computer interface," *Comput. Intell. Neurosci.*, p. 37695, 2007.
- [43] B. Blankertz, R. Tomioka, S. Lemm, M. Kawanabe, and K. R. Müller, "Optimizing spatial filters for robust EEG single-trial analysis," *IEEE Signal Process. Mag.*, vol. 25, no. 1, pp. 41–56, 2008.
- [44] D. J. Krusienski *et al.*, "Critical issues in state-of-the-art brain-computer interface signal processing," *J. Neural Eng.*, vol. 8, no. 2, p. 025002, Apr. 2011.
- [45] J. N. Mak *et al.*, "Optimizing the P300-based brain-computer interface: Current status, limitations and future directions," *J. Neural Eng.*, vol. 8, no. 2, p. 025003, Apr. 2011.
- [46] G. Pfurtscheller, J. Kalcher, C. Neuper, D. Flotzinger, and M. Pregener, "On-line EEG classification during externally-paced hand movements using a neural network-based classifier," *Electroencephalogr. Clin. Neurophysiol.*, vol. 99, pp. 416–425, Nov. 1996.
- [47] N. J. Huan and R. Palaniappan, "Neural network classification of autoregressive features from electroencephalogram signals for brain-computer interface design," *J. Neural Eng.*, vol. 1, pp. 142–150, Sep. 2004.
- [48] R. Millan Jdel, F. Renkens, J. Mouriño, and W. Gerstner, "Noninvasive brain-actuated control of a mobile robot by human EEG," *IEEE Trans. Biomed. Eng.*, vol. 51, no. 6, pp. 1026–1033, Jun. 2004.
- [49] G. Pires, M. Castelo-Branco, and U. Nunes, "Visual P300-based BCI to steer a wheelchair: A Bayesian approach," in *Proc. IEEE Eng. Med. Biol. Soc. Conf.*, 2008, pp. 658–661.
- [50] B. Blankertz, S. Lemm, M. Treder, S. Haufe, and K. R. Müller, "Single-trial analysis and classification of ERP components—A tutorial," *Neuroimage*, vol. 56, no. 2, pp. 814–825, May 2011.

Sui Man Lai (M'11) was born in Hong Kong, in 1985. He received the B.Eng. (Hons) degree in medical engineering in 2007, and the M.Phil. degree in electrical and electronic engineering from the University of Hong Kong, Pokfulam, Hong Kong.

He is now with the Neuroengineering Laboratory at University of Hong Kong and working as a Research Engineer. He is interested in developing novel methods and applications in brain-computer interface.

Zhiguo Zhang (S'05–M'07) received the B.Sc. degree in electrical and electronic engineering from Tianjin University, Tianjin, China, in 2000, the M.Eng. degree in electrical and electronic engineering from the University of Science and Technology of China, Hefei, China, in 2003, and the Ph.D. degree from the Department of Electrical and Electronic Engineering, The University of Hong Kong, Pokfulam, Hong Kong, in 2008.

He is currently a Research Assistant Professor with The University of Hong Kong. His research interests include biomedical signal processing, neural engineering, and computational neuroscience.

Yeung Sam Hung (M'88–SM'02) received the B.Sc. (Eng.) degree in electrical engineering and the B.Sc. degree in mathematics from the University of Hong Kong, Pokfulam, Hong Kong, and the M.Phil. and Ph.D. degrees from the University of Cambridge, Cambridge, U.K.

He was a Research Associate with the University of Cambridge and a lecturer with the University of Surrey, Surrey, U. K. In 1989, he joined the University of Hong Kong, where he is currently a Professor. His current research interests include robust control and filtering theory, system modeling, robotics, computer vision, biomedical engineering, and bioinformatics.

Zhendong Niu received the Ph.D. degree in computer science from Beijing Institute of Technology, Beijing, China, in 1995.

He was a post-doctoral researcher at University of Pittsburgh, Pittsburgh, PA, from 1996 to 1998, and a researcher/adjunct faculty member at Carnegie Mellon University, Pittsburgh, PA, from 1999 to 2004, and a joint research professor at the Information School of University of Pittsburgh from 2006. He received IBM Faculty innovation Award in 2005 and was awarded New Century Excellent Talents in University of MOE of China in 2006. He is Professor and Deputy Dean of the School of Computer Science and Technology at Beijing Institute of Technology. His research areas focus on web-based learning techniques, informational retrieval, digital libraries, neuroinformatics, software architecture, etc. He serves as editorial board member for *International Journal of Learning Technology* and many other journals. He has published more than 80 papers in journals and international conferences.

Chunqi Chang (M'06) received the B.Sc. (Eng.) and the M.Sc. (Eng.) degrees in electronic engineering from the University of Science and Technology of China, Hefei, China, in 1992 and 1995, respectively, and the Ph.D. degree in biomedical engineering from the University of Hong Kong, Pokfulam, Hong Kong, in 2001.

Since 2002, he has been with the Department of Electrical and Electronic Engineering, University of Hong Kong, where he is currently a Research Assistant Professor. His research interests are in the areas of signal processing and machine learning with applications in biomedical engineering and bioinformatics, particularly statistical signal processing, blind signal processing, computational neuroscience and neuroengineering, brain computer interface, event-related brain potentials, and computational systems biology.